

In-situ vibration tests and numerical analysis of embedded foundations

Shozo Katano & Tamotsu Ogawa
Tokyo Electric Power Co., Japan

ABSTRACT: This paper examines the effects of embedded box-shaped foundations based on data obtained from in-situ vibration tests and numerical analyses. As a result, it was concluded that the damping effect increases with foundation embedment and that it is possible to simulate fairly closely the damping effects of foundation embedment using the axi-symmetric finite element method.

1 INTRODUCTION

The foundation upon which the tests were conducted was designed to support a synchronous phase modifier, a type of synchronous machine (see Figure 1) used to stabilize electric power transmission networks. The foundation was to eventually support a 5100 kN (rotor: 2750 kN) synchronous phase modifier, which rotates at a speed of 600 rpm on a vertical axis.

The foundation under investigation was built on quarternary ground. Early in the foundation designing stages there was some concern that resonance may occur between the synchronous phase modifier and the foundation if the

foundation was laid above the ground. As a result of this concern, an embedded foundation was adopted in order to reduce vibrations within the foundation.

This paper contains the results of vibration tests and numerical analyses which were both devised to confirm the effects of foundation embedment as well as the validity of the vibration prediction method applied during the designing stages of the foundation.

2 VIBRATION TESTS

2.1 Foundation Structure, Geological Conditions, Test Methods

The foundation (see Figure 2) upon which the vibration tests were conducted was completely embedded and box-shaped. The surrounding soil consisted of a two-meter banking layer (shear wave velocity: $V_s=75-160$ m/s) and a three-meter loam layer ($V_s=160$ m/s) followed by a thick layer consisting mainly of gravel ($V_s=400-700$ m/s). Each soil layer was more or less horizontal. The vibration tests were conducted at different stages (ie. two different heights) of the foundation's construction:

(1) After completion of the base slab (height: 4.2 m, weight: 31,500 kN)

(2) After completion of the foundation (height: 10.0 m, weight: 55,900 kN)

Vibrations of 3.0 to 15.0 Hz were applied at 0.2 Hz intervals along the lengthwise direction of the foundation. The vibration generator used had a maximum vibrating force of 98 kN and was set in the same position during both testing stages. The foundation was constructed using the soldier pile and lagging method. After completion of the base slab, the vertical face of soil extending from the top of the base slab to the ground surface was supported with a retaining wall.

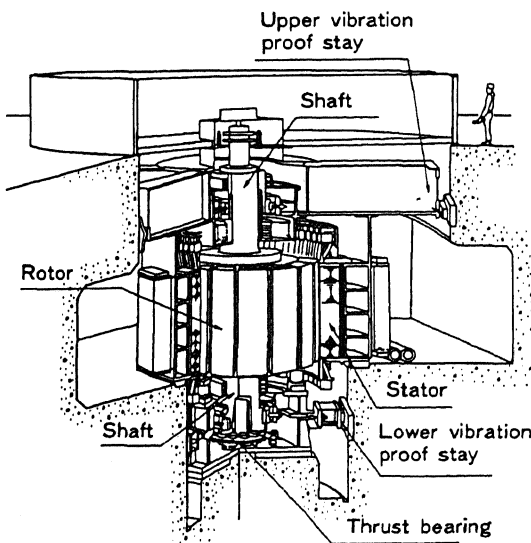
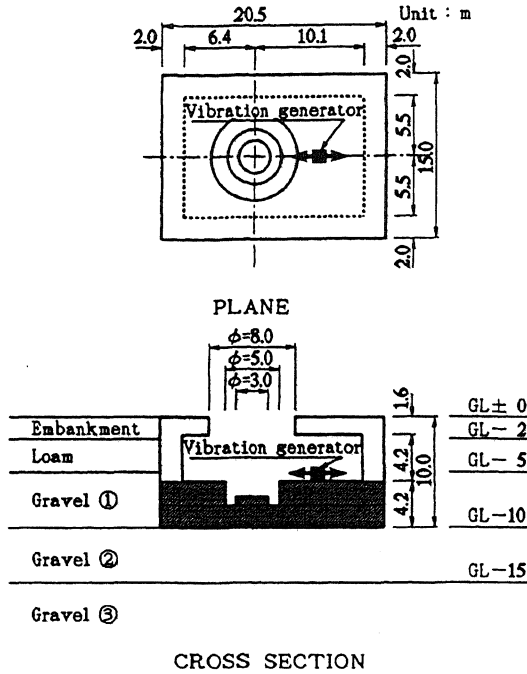


Figure 1. Outline of synchronous phase modifier



Layer	Depth (m)	Unit weight γ_s (kN/m ³)	Shear wave velocity V_s (m/s)
Embankment	0~2	13.8~15.0	75~160
Loam	2~5	13.4~15.2	160
Gravel ①	5~10	19.1~22.4	400
Gravel ②	10~15	-	600
Gravel ③	15~	-	700

Figure 2. Outline of foundation and soil profile

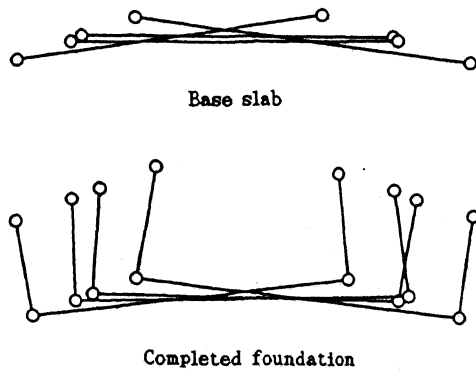


Figure 3. Mode shape of foundation (8Hz).

2.2 Results

As can be seen in Figure 3, the foundation's vibration movements were that of a rigid body with two degrees of freedom (swaying and rocking) during both testing stages.

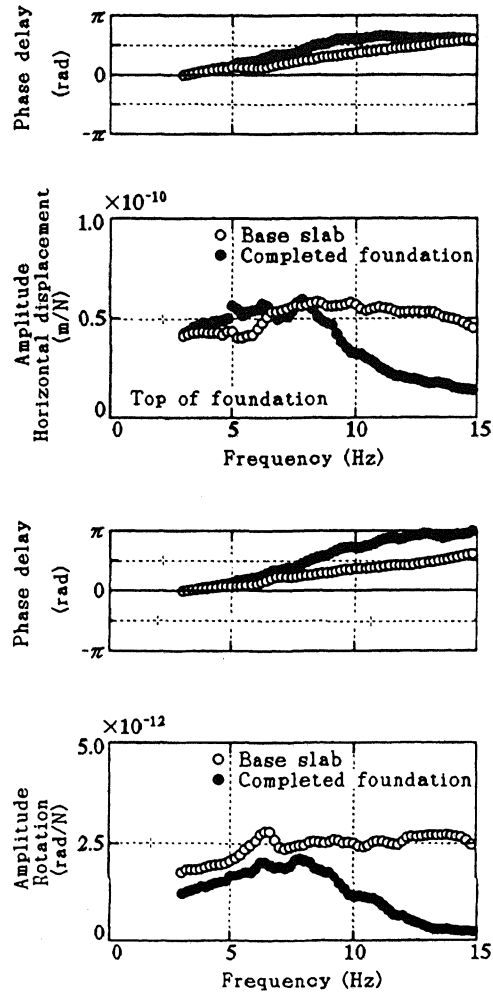


Figure 4. Resonance curves.

The foundation's horizontal displacement and rotation resonance curves (see Figure 4) also have no main peak. Small peaks at 6 and 8 Hz can be seen in the resonance curves taken after completion of the foundation. These peaks are thought to correspond with the 5.7- and 7.0 Hz microtremor predominant frequencies measured in the upper ground layers (see Figure 5). In the numerical analyses, a peak of 6.0 Hz was calculated as the predominant frequency for the ground lying above GL -15 meters, and a peak of 8.0 Hz was calculated to be the predominant frequency for ground lying above GL -5 meters. The 9.3 Hz microtremor peak is due to the slower shear wave velocity at the point of measurement. The shear wave velocity for the ground lying above GL -2 meters was measured to be $V_s = 160$ m/s at the foundation location but stood at $V_s = 75$ m/s at the microtremor measuring point (see section 3.1). Comparison of the resonance curves for both stages reveals that the high frequency (frequencies above 10 Hz) responses measured after foundation com-

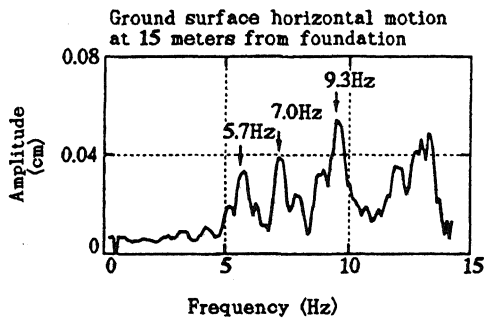


Figure 5. Fourier spectrum of microtremor measurement.

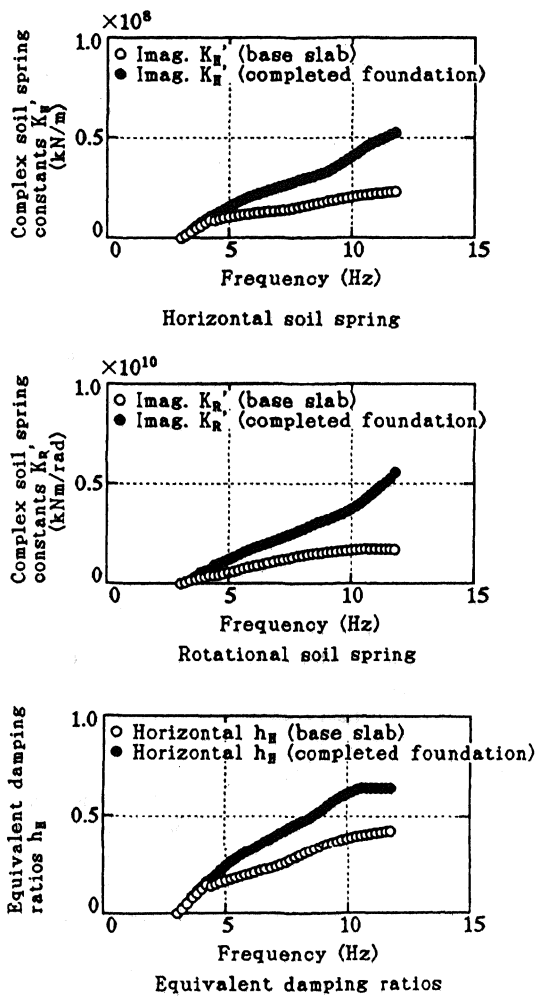


Figure 6. Complex soil constants and equivalent damping ratios.

pletion are much lower than those measured after the completion of the base slab.

2.3 The Effects of Embedding Foundations

In order to understand clearly the effects of embedding the foundation as indicated by the vibration test results, the interaction between the ground and the foundation was represented by complex soil springs which were given values calculated from the vibration test response results. The resultant analytical model was given two degrees of freedom (Novak 1972, Harada 1981) in accordance with the foundation vibration mode ascertained in the vibration tests. Complex springs with horizontal and rotational components were also attached to the underside of the foundation. Figure 6 indicates the complex soil springs derived from each vibration frequency. The imaginary parts of the complex springs in figure 6 indicate the damping aspects of the foundation. The figure indicates that the values for the complex spring imaginary parts increase with the increase in frequency, and that the imaginary number values for the point of completion of the foundation are almost double those for the point of completion of the base slab.

A similar trend can be observed for the equivalent damping ratios calculated from the real and imaginary parts of the complex springs. Judging from the above results, it was concluded that the reason the response amplitude measured after the completion of the foundation was much lower than that measured after completion of the base slab was due to the interaction between the foundation side wall and the surrounding soil. In other words, the foundation side wall increased the damping ability of the foundation and effectively reduced the response amplitude of the foundation.

3 NUMERICAL ANALYSES

3.1 Investigation of the Validity of Axi-symmetric FEM Models

Although an axi-symmetric model was used to estimate vibration in the foundation's designing stages, a comparison between the test and numerical analysis results was carried out to confirm the validity of analyses using an axi-symmetric model. The model (see Figure 7) was based on the assumption that the surrounding soil was horizontal. Within the model, the foundation was represented as a cylinder with an undersurface equal to that of the foundation's square undersurface. The semi-infiniteness of the ground was represented by an energy transmitting boundary (Lysmer, 1972) along the sides of the ground and a viscous boundary (Lysmer, 1966) along the bottom of the ground. The Ground property values used were those shown in Figure 2. The banking

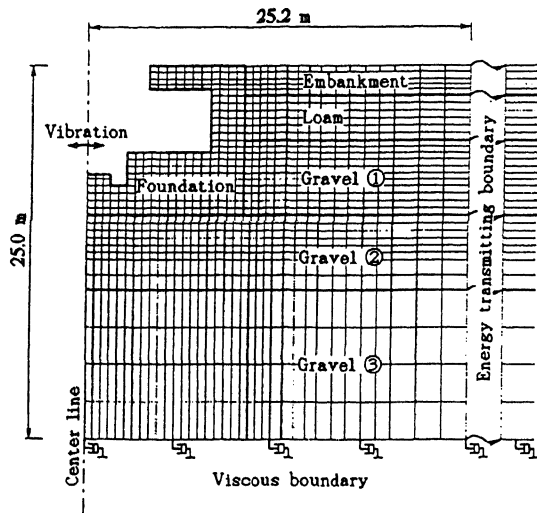


Figure 7. Axi-symmetric FEM model.

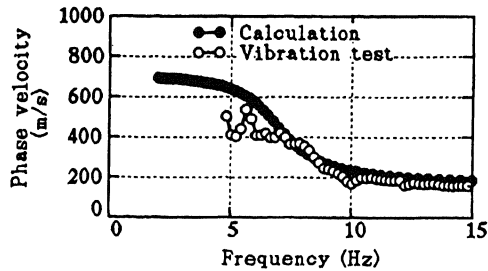


Figure 8. Dispersion curve.

layer shearing wave velocity was set at 160 m/s (see Figure 8). This was determined after comparing the Love wave dispersion curve analysis value with the wave motion phase velocity obtained from the vibration test soil response results. Figure 9 compares the results of the vibration test with the calculated FEM results for the top of the foundation and the ground surface (15 meters from foundation). The figure shows that the FEM calculated results closely correspond with the vibration test response curves for the foundation and surrounding soil.

3.2 Investigation into the Effects of Embedding Foundations According to the Axi-symmetric FEM Model Results.

As the foundation was embedded during both stages of the vibration tests, it was difficult to evaluate the damping effects of the foundation in comparison with those of a foundation laid above the ground surface. Numerical analyses using an axi-symmetric FEM model were therefore carried out in order to investigate the effects of embedding the foundation.

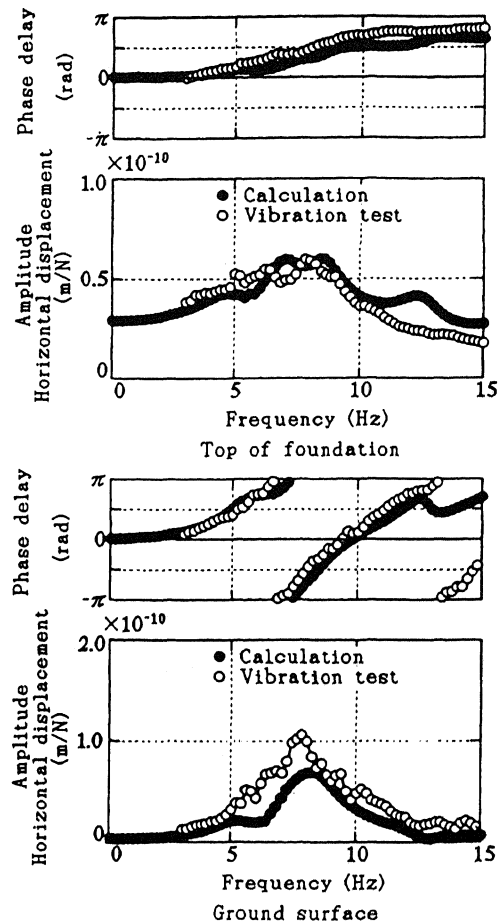


Figure 9. Comparison of resonance curves between calculation and vibration test.

Analyses were carried out for the following three cases:

- (1) Completely Embedded: The same model as described in section 3.1 (see Figure 7).
- (2) Half Embedded: Model with the top five meters of soil removed (see Figure 10).
- (3) Exposed: Model with the top 10 meters of soil removed (see Figure 11).

Analysis results indicated clearly the effects of embedding the foundation which was something that was not made clear in the vibration tests. The maximum foundation amplitude became smaller depending on the embedded depth. This can be clearly seen in the differences in the amplitudes for the completely embedded, half embedded and exposed foundation when subject to frequencies of 8.6 Hz (see Figure 12). The foundation displacement values obtained in the above analyses were then used to obtain the complex soil springs and equivalent damping ratios for the foundation in its completely embedded and exposed state (see Table 1). From the table, it can be observed that the ground surrounding the foun-

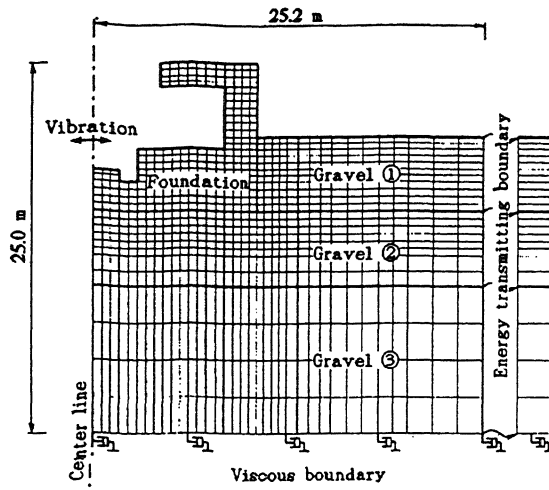


Figure 10. Axi-symmetric FEM model (Half embedded)

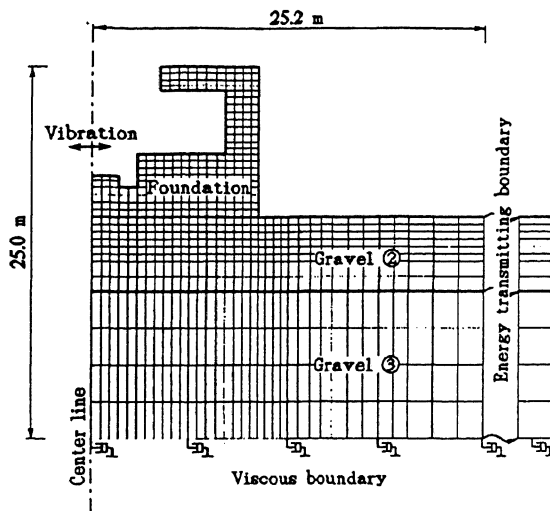


Figure 11. Axi-symmetric FEM model (Exposed)

dation does help to damp vibrations within the foundation (indicated in the row marked "equivalent damping ratios") even though the spring effect of this ground is small.

4 CONCLUSION

The embedded foundation vibration tests and numerical analyses resulted in the following valuable findings:

(1) From the results of the vibration tests it was concluded that the interaction between the foundation wall and the surrounding soil helps to greatly improve the foundation's damping ability as well as reduce the re-

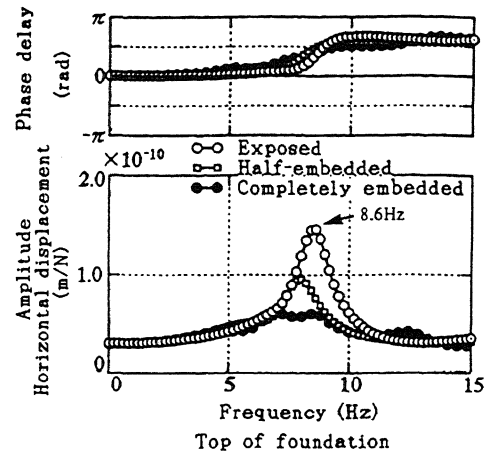


Figure 12. Numerical analysis resonance curves.

Table 1. Complex soil spring constants and equivalent damping ratios (based on numerical analysis results; 8.6Hz)

		Completely embedded	Exposed
Horizontal soil spring constants	Real K_H (kN/M)	2.9×10^7	2.9×10^7
	Imaginary K_H' (kN/M)	2.8×10^7	1.2×10^7
Rotational soil spring constants	Real K_R (kNm/rad)	2.8×10^9	2.1×10^9
	Imaginary K_R' (kNm/rad)	1.6×10^9	0.7×10^9
Equivalent damping ratios	Horizontal h_H (%)	40	19
	Rotational h_R (%)	26	17

sponse amplitude. These effects are especially noticeable in the high vibration frequency regions.

(2) Comparison of the vibration test and numerical analysis results revealed that by using an axi-symmetric model, it is possible to represent fairly closely, a box-shaped foundation as well as ground responses to applied vibration.

(3) Investigation of the effects of foundation embedment according to the numerical analyses results revealed that the foundation damping ability increases with the level of backfill, and that complete embedment results in a disappearance of an obvious peak in the resonance curve. A similar phenomenon was observed during the vibration tests.

ACKNOWLEDGEMENTS

We would like to thank Dr. Keizaburo Kubo, an honorary professor of The University of Tokyo for his guidance with the analyses, as well as all other parties who assisted in the project.

REFERENCES

- Harada, T. et al., 1981. Dynamic Soil-structure Interaction Analysis by Continuum Formulation Method, The University of Tokyo Institute of Industrial Science Report, Vol. 29, No. 5
- Lysmer, J. et al., 1966. Dynamic Response of Footings to Vertical Loading, Proc. ASCE Vol. 92 No. SMI: 65-91
- Lysmer, J. et al., 1972. A Finite Element Method for Seismology, Methods of Computational Physics, Vol. 11, Academic Press
- Novak, M. et al., 1972. Coupled Horizontal and Rocking Vibration of Embedded Footings, Canadian Geotechnical Journal, Vol. 9